Robin Amacher, Théodora Cohen Liechti, Ph.D., Michael Pfister, Dr.Sc., Giovanni De Cesare, Dr.Sc. and Anton J. Schleiss, Dr.Sc.
Laboratory of Hydraulic Constructions (LCH), Ecole Polytechnique Fédérale de Lausanne (EPFL),
CH-1015 Lausanne, Switzerland

Wave-reducing Stern Flap on Ship Convoys to Protect Riverbanks

ABSTRACT

Inland navigable waterways are significant in cargo transport and leisure activities. In parallel, these channels and rivers often suffer from the ship traffic, as the generated waves may damage waterway banks, along with their riparian fauna. As a consequence, speed limits have commonly been introduced. In some cases, adaptations on the vessel might be more appropriate as an alternative. This paper describes a flap that is mounted at the stern of a barge and is operated by a pusher tug. The barge is used to transport around 170 tons of waste per course from the City of Geneva (Switzerland) to an incineration plant. The optimum shape of the flap was derived from numerical and physical modeling, and its effect tested in situ. The latter indicated that, on site, the wave energy at 20 m distance to the convoy was reduced by half with the use of the flap.

INTRODUCTION

The domestic waste of the City of Geneva (Switzerland) is transported on the Rhone River from the city to the waste incineration station—located outside of the city— with ship convoys. They consist of a 12.1 m long and 5.5 m wide pusher tug, and a 43.0 m long and 8.6 m wide barge (Figure 1) that is operated by the Industrial Services of Geneva (SIG). Waves generated by these convoys affect the river banks and the riparian fauna. To reduce the impact of the convoy passages on the banks and fauna, the SIG assigned the Laboratory of Hydraulic Constructions (LCH) of Ecole Polytechnique Fédéral de Lausanne (EPFL) to analyze the situation and to propose modifications on the convoy to minimize the wave impact.

FIGURE 1. Pusher tug and barge on Rhone River, travelling upstream with approximately V_r = 4.2 m/s.

The impact on the banks can be limited by reducing the wave energy and thus its height (Bishop 2003, Glamore 2008), which also affects bank erosion (as reported by Nanson et al. 1994) as well as fauna (as mentioned by Coops et al. 1996, and Bishop and Chapman 2004). Furthermore, travelling vessels also affect sediment re-suspension near the embankments (De Roo et al. 2012).

The wave system generated by a ship has a spectrum of waves: the shortest wave is infinitesimal and the longest depends on the speed of the ship. Three approaches exist to reduce the wave height generated by a vessel: (1) an adaptation of the hull shape, (2) a reduction of the convoy velocity, and (3) an increase of the vessel length. The approaches (2) and (3) are characterized by the Froude number (e.g., Froude 1877) defined as

$$F = \frac{V_r}{\sqrt{gL}} \qquad (1)$$

where V_r = convoy velocity relative to surrounding water, g = acceleration due to gravity, and L = vessel length. The wave type and height generated by a vessel is linked to F. For F<0.15, the wave drag is relatively small (Presles and Paulet 2005, Blevins 1984, Newman 1977). As F increases, the resulting wave length also increases, finally reaching L for F= 0.4, considered limit velocity for displacement type vessels. For higher velocities (resulting in larger values of F), the wave drag becomes dominant, increasing faster than the viscous drag.

For the presented case, a reduced convoy velocity is not appropriate for logistical reasons and a hull adaption is too complex. The increase of L is, however, is feasible by "linking" the pusher tug and the barge hydrodynamically by adding a stern flap to the barge. Table 1 gives F in function of L and for two characteristic V_r (Table 2), indicating that a hydrodynamic connection of the pusher tug and the barge (resulting in a convoy) reduces F, particularly to values close to F= 0.15.

Based on both the numerical and physical model testing, a flap mounted at the barge stern resulted as the most efficient method of reducing the wave energy (linked to the dominant wave occurring at the barge stern). The latter concept is frequently applied for ship stability, powering improvements, and wave height reduction for powerboats (e.g., Cusanelli and Hundley 1999), but hardly to hydrodynamically "connect" two vessels. The flap is operated by hydraulic cylinders and lowered during journey, but is lifted up in port to facilitate maneuvers.

	Pusher tug	Barge	Convoy
V_r [m/s]	L=12.1 m	L=43.0 m	L=55.1 m
3.25	0.30	0.16	0.14
4.31	0.40	0.21	0.19

TABLE 1. Values of Froude number for different vessel length L and velocity V_r.

SIG owns one pusher tug and four barges, one of which was equipped with the recommended flap. To verify the efficiency of the flap, SIG appointed LCH with in situ measurements of the wave trains generated by two types of barges: (1) with flap, and (2) without flap. From this point, the effect of the flap will be described, as the design is a secondary issue.

Design of the flap

MODELING

Physical model tests and numerical simulations were conducted to find an efficient flap shape (LCH 2009). The tests and simulations did not include the effective Rhone River situation, but were set up to allow for a relative comparison of the tested flaps in terms of their effect on the generated waves. It should be noted that eventual scale effects occurring in the physical model as well as simplifications in the numerical modeling (e.g., overestimated wave diffusion, Muk-Pavic et al. 2006) are of minor relevance, as a comparative study was conducted.

The *physical model* tests were conducted at 1:30 scale, based on the Froude similitude (Figure 2a). The hull of the pusher tug and the barge were both modeled using polystyrene foam. The ship models were loaded to adjust the gravity center as well as inertia, and were painted to smooth their surface. The pusher tug was connected to the barge by two rods that allowed movement along the vertical axis as well as pitch rotation. The tests were conducted in a 2 m wide and 47 m long channel, regulating the flow depth (typically 0.185 m in the model, equivalent to 5.55 m in prototype) with a shutter gate at the channel end. The channel discharge was supplied by in-house pumps and was measured using a Magnetic Inductive Discharge Meter. The convoy was fixed on a motor-driven trolley with velocity control and measurement, which pulled the convoy along the channel. The model Reynolds numbers were at minimum $7.7 \cdot 10^5$ with the barge length as reference, and $2.2 \cdot 10^5$ for the pusher. The static water levels, as well as the wave profiles, were measured using Ultrasonic Distance Sensors (UDS, Baumer UNAM 30) installed transversally across the channel at 0.23, 0.40, and 0.80 m distance to the stream-wise axis

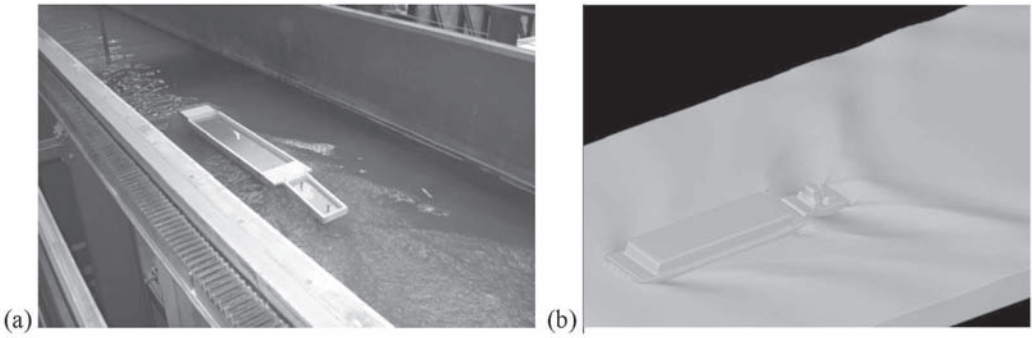

FIGURE 2. (a) Physical and (b) numerical model showing convoy passage.

of the convoy. The channel bottom cross-section was rectangular. The water depth was constant, whereas variable "river" discharges and vessel velocities were tested.

The *numerical simulation* was set up with Flow-3D (Figure 2b), solving the continuity and momentum equations with a finite-volume approximation. The flow region was subdivided into a mesh of fixed rectangular cells with a spacing of 0.29 m in a stream-wise direction, 0.21 m transversally and 0.13 m vertically near the convoy. At the center of the cells, local averages of all dependent variables are associated, except for velocities being located at the cell faces (staggered grid arrangement). The channel boundaries, as well as the pusher and the barge, were embedded by defining the fractional face areas and fractional volumes of the cells that are open to flow (FAVOR method). The two-equation k-ε model is used for turbulence closure. The single incompressible fluid with a free surface model was used with no-slip condition on any solid surface boundary (i.e., the river bottom, pusher tug, and barge). The 3-D geometry of the pusher tug and barge were inserted as two stereo-lithography (STL) files, approximating the surfaces by triangles.

The numerical simulations included the following configurations: (*i*) four small identical bulbs at the barge, one at each corner, (*ii*) the herein described "long" (4.50 m in course direction) barge stern flap, (*iii*) short pusher stern flaps (0.50 and 1.00 m in course direction), and (*iv*) a stern flap at the pusher as well as at the barge (between 1.00 and 4.50 m in course direction). These configurations were compared with the original situation, i.e. without any installation. The simulated wave heights (for V_r = 6.7 m/s to overestimate the effect, derived at D = 5.11 m) indicated that the bulbs and the pusher flap were less effective, whereas the barge flap significantly reduced the wave heights generated at the barge stern and the pusher bow. Then, the physical experiments were conducted to verify the numerical simulations, and to further specify the effect of the different configurations, varying the flap length, angle relative to the horizontal, and thickness. Each configuration was tested under various V_r. The retained optimum configuration is described hereafter, considering the effect on the wave heights beside constructional and operational aspects (LCH 2009).

OPTIMUM SHAPE

The aforementioned experiments indicated that a barge stern flap (4.50 m long, in stream-wise direction) and 8.60 m wide (transversally, identical to the width of the flat barge hull portion) is optimal, being horizontally aligned with the barge bottom (figures 3 and 4). In order to lift the flap for maneuvers, its maximum length is restricted by the pusher fittings.

FIGURE 3. Optimum flap location, shape, and angle.

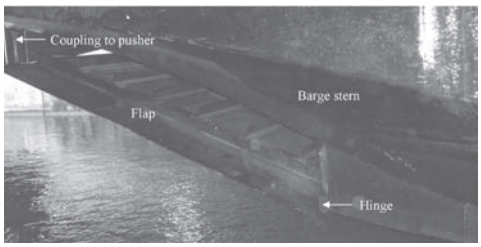

FIGURE 4. Photo of the flap at the barge stern in elevated position to allow for maneuvering.

Scenario	Modified barge, with flap				Original barge, without flap			
	Test no.	D [m]	V_a [m/s]	V_r [m/s]	Test no.	D [m]	V_a [m/s]	V_r [m/s]
Against stream, slow (AS)	1	4.3	2.19	3.17	5	1.9	2.28	3.25
With stream, slow (WS)	10	0.7	4.22	3.25	6	3.9	4.22	3.25
Against stream, fast (AF)	3	4.4	3.25	4.22	7	2.4	3.33	4.31
With stream, fast (WF)	4	4.6	5.31	4.33	8	2.3	5.22	4.25

TABLE 2. Tested scenarios (D = distance between barge hull and UDS 1, V_a = absolute convoy velocity relative to ground, and V_r = convoy velocity relative to surrounding water).

In Situ Validation

TEST SETUP

A straight reach of the Rhone River with a stream-wise regular cross-section of some 90 m width was chosen for the in situ tests (LCH 2011). The Rhone River discharge was 390 m^3/s, measured by the gauging station "Chancy". The flow velocity was measured at the water surface in the river center using Acoustic Doppler Velocimetry (OTT Nautilus C2000) as 0.98 m/s, and the maximum flow depth at the Talweg was derived as 7.0 m from the bathymetry and water surface data. The absolute velocity of the convoy was measured using on-board GPS, as well as implicitly by Laser Distance Sensor (LDS).

To record the wave trains generated by the convoy, a 20 m long beam was suspended below the bridge "Passerelle du Lignon" (Figure 5). The latter was equipped with four vertical UDS (Baumer UNAM S14) to record the water surface (wave profiles), and a horizontal LDS (Micro-Epsilon ILR) to derive the distance between the UDS and the convoy. The effective distance D between the UDS and the barge hull slightly varied at every passage, as the convoy was difficult to navigate precisely. Therefore, the latter varied in the order of D = 2 to 4 m for the closest UDS no. 1. The other UDS were fixed at distances of (2) D+2 m, (3) D+7 m and (4) D+20 m toward the bank. The UDS no. 4 was thus closest to the riverbank, with a remaining distance of approximately 20 m to the bank.

The test program is given in Table 2, with V_a = absolute convoy velocity relative to ground. Four basic scenarios were considered, each with and without the flap to allow for comparison. The other parameters (i.e., D, V_a, V_r, and weight of the convoy) were kept as constant as possible within the scenario, to exclude their influence on the waves.

FIGURE 5. In situ test setup showing the suspended measurement beam below the bridge and convoy after passage, travelling upstream.

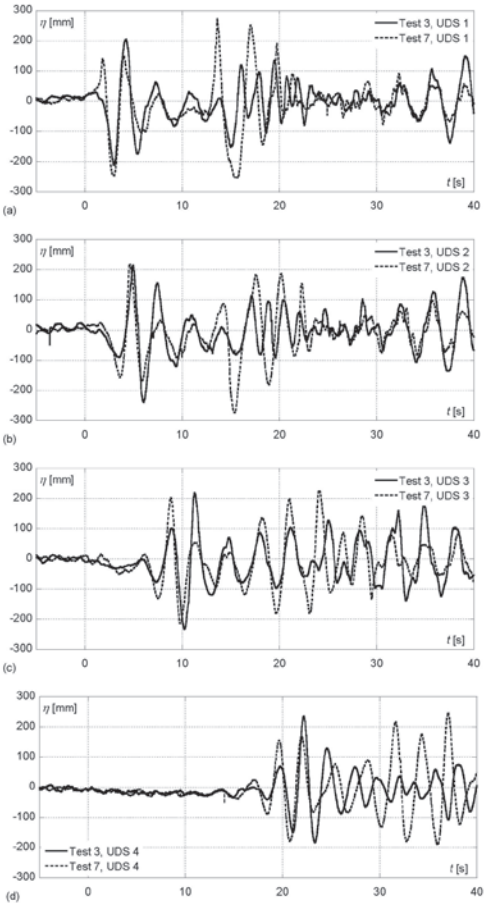

FIGURE 6. Wave profiles characterized by vertical surface displacement η for scenario AF (against stream fast, Table 2), i.e., Tests 3 with flap (—) and Test 7 without flap (---), measured at UDS (a) 1 (near convoy), (b) 2, (c) 3, and (d) 4 (near riverbank).

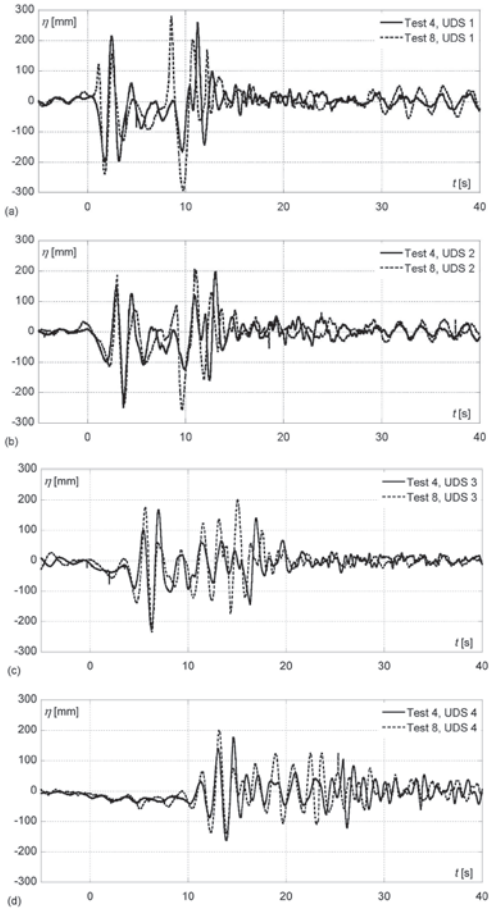

FIGURE 7. Wave profiles characterized by vertical surface displacement η for scenario WF (with stream fast, Table 2), i.e., Tests 4 with flap (—) and Test 8 without flap (---), measured at UDS (a) 1 (near convoy), (b) 2, (c) 3, and (d) 4 (near riverbank).

EFFECT ON WAVE TRAIN

Figures 6 and 7 show the wave trains as a function of time for the scenarios AF and WF (Table 2: against and with the stream, fast passage), comparing the passages with and without flap. Here, η = vertical water surface displacement relative to still water elevation (at η=0 m). Figures 6(a) and 7(a) show the waves at UDS 1, i.e. close to the convoy; Figures 6(b) and 7(b) at UDS 2; figures 6(c) and 7(c) at UDS 3; and figures 6(d) and 7(d) show the waves at UDS 4, i.e., close to the riverbank.

The waves near the convoy (UDS 1, figures 6a and 7a) mainly depend on its geometry. The first wave package corresponds to the bow wave of the barge, which remains similar in terms of frequency and amplitude for all passages (during 1 s≤t≤6 s in Figure 6a, lower left in Figure 1). Then, during the passage of the barge, reduced wave heights are observed as shown in Figure 6a for roughly 6 s≤t≤12 s. The second wave package, including the dominant amplitudes to reduce, is generated at the barge stern and at the pusher bow (during 12 s≤t≤22 s in Figure 6a, lower right in Figure 1). For the original barge, the stern of the barge generates a wave sent to and amplified by the pusher bow by interference. With the flap, the stern wave of the barge is delayed, so that the resulting wave is flattened. After the passage (t>22 s in Figure 6a), the pusher stern and wake wave follow, with some interferences generating considerable wave amplitudes. With increasing distance from the convoy (UDS 4, Figures 6d and 7d), the link between convoy elements

and the resulting waves becomes less obvious, whereas the damping effect of the flap remains.

EFFICIENCY REGARDING WAVE ENERGY

The principal aim of this investigation was to reduce the total wave energy impact on riverbanks, beside a reduction of the maximum amplitudes. The latter is difficult to quantify but generally achieved, as can be seen in Figures 6 and 7.

As the wave profiles indicate, the typical wave length l is around 12 m, the maximum water depth W around 7 m, and the maximum wave height H around 0.4 m. Then, H/W=0.06, $(H/l)(l/W)^3$=0.168, and W/l=0.58. Besides, the depth-related Froude number is always smaller than 0.6 at the position of all UDS, so that finite-depth effects are of minor importance for wave-making. The herein observed waves are thus a priori linear deep water waves (Le Méhauté 1976, Newman 1977), so the linear small amplitude wave theory applies. The total wave energy E per unit width according to Dean and Dalrymple (2004) is then

$$E = \frac{1}{8}\rho g H^2 l \qquad (2)$$

with ρ= water density. The wave energy is thus proportional to the square of the wave height. Ippen (1966) proposes for complex wave trains the integration of η^2 over time t, so that

$$E = f\left(\int \eta^2 \mathrm{d}t\right) \qquad (3)$$

Herein, all wave parameters except the vertical surface displacement η are thus considered as constant between two related scenarios. Note that l, particularly, is a function of V_r, which was almost identical between the two related scenarios.

The relative remaining wave energy P is compared between two associated scenarios based on Eq. (3), with $P=E_m/E_o$. The subscript m refers the modified barge (including tests no. 1, 10, 3, and 4), and the subscript o to the original barge

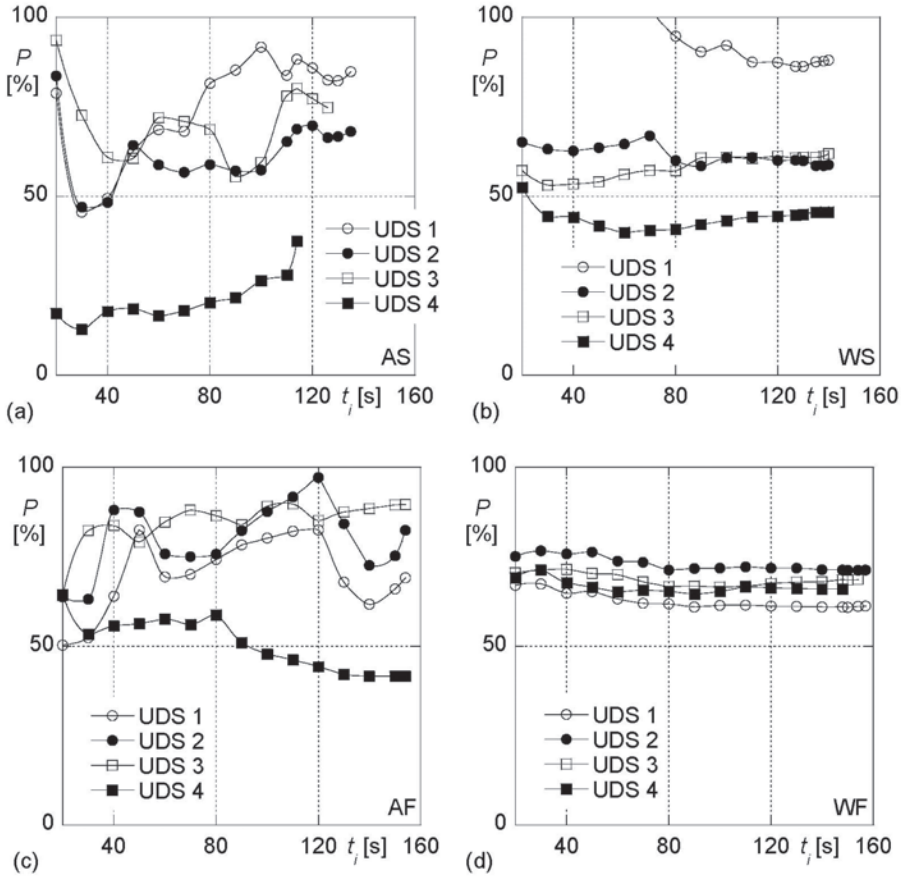

FIGURE 8. Relative remaining wave energy P (ratio with/without flap) versus upper integration time limit t_i, at different UDS (1 near convoy, 4 near riverbank) for the scenarios (a) AS, (b) WS, (c) AF, and (d) WF.

(including tests no. 5, 6, 7, and 8). The integration time was between $t = 0$, i.e., when the first ship-generated wave was recorded, and $t = t_i$ as upper limit. The latter was chosen to reproduce eight times the convoy length for slow passages, and 12 times for fast passages. The background wave noise was removed prior to the integration, based on a reference noise measurement. As seen in Figure 8, the t_i values affect P. Nevertheless, the overall trend of the P-curves is generally stable and *a priori* constant, so that an average of the P-values shown in Figure 8 (with 20 s$\leq t_i \leq$110 s) is used for the further summary (Figure 9).

Figure 9 shows the relative remaining wave energy P at different UDS for the scenarios defined in Table 2. For scenario WF, for example, $P=E4/E8=0.67$ at UDS 4, indicating that the passage with the flap generates waves with only 67% of the energy of the original barge. Vice versa, the wave energy closest to the riverbank was reduced by some 33% due to the flap. Note that $P>100\%$ at UDS 1 for scenario WS and for $t_i<80$ s, as $D=0.7$ m for the passage of the modified barge, and $D=3.9$ m for the original barge. The modified barge was thus much closer to UDS 1, so that a comparably higher wave was recorded. On average, the remaining energy of the modified convoy is 77% as compared to the non-modified at UDS 1, 69% at UDS 2, 71% at UDS 3, and 46% at UDS 4. Thus, the sensor closet to the riverbank (UDS 4) indicates a wave energy of the modified convoy, which is around half that of the non-modified convoy.

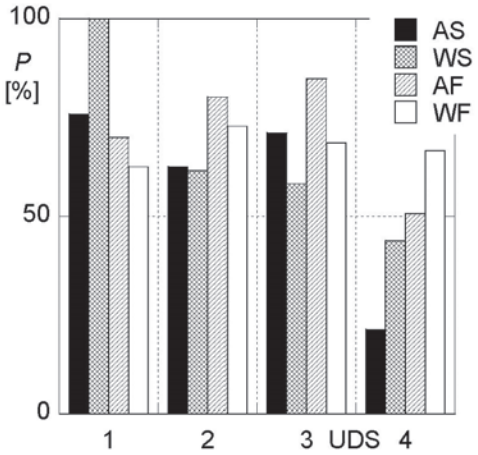

FIGURE 9. Values P at different UDS for the scenarios defined in Table 2 (average of all P values with 20 s$\leq t_i \leq$110 s).

Conclusions

Numerical simulations and physical model tests were conducted to verify the effectiveness of a flap mounted on a barge stern to hydrodynamically "connect" the latter to the pusher tug. According to theory, this should result in a reduction of the generated wave height, thereby also decreasing the remaining wave energy being dissipated onto the riverbanks. Modifications on the convoy were requested to limit wave damage to riverbanks without the need to place a limitation on operational speed. Preliminary-conducted numerical simulations and physical model tests showed that bulbs, short flaps, and an arrangement of several flaps were less effective than a single large flap mounted at the barge stern. The effective in situ performance of the latter was thereafter tested with a comparison of a convoy with an original barge and a convoy with a modified barge. The measurements of the wave trains indicated that the barge with a flap generated reduced integral wave energy for all tested scenarios. At 20 m distance from the convoy axis, it even reduced the wave energy on average by some 50%.

ACKNOWLEDGEMENTS

The Authors thank the Industrial Services of Geneva (SIG) for the excellent collaboration, in particular Mr. Jan Stefanski.

REFERENCES

Bishop, M.J. (2003). *Making waves: the effects of boat-wash on macrobenthic assemblage of estuaries.* Ph.D. Thesis, University of Sydney.

Bishop, M.J., Chapman M.G. (2004). Managerial decision as experiments: an opportunity to determine the ecological impact of boat-generated waves on macrobenthic in fauna. *Estuarine, Coastal and Shelf Sciences*, 61(4), 613-622.

Blevins, R.D. (1984). *Applied Fluid Dynamics Handbook*. Van Nostrand Reinhold, New York.

Coops, H., Geilen, N., Verheij, H.J., Boeters, R., van der Velde, G. (1996). Interactions between waves, bank erosion and emergent vegetation: an experimental study in a wave tank. *Aquatic Botany*, 53(3-4), 187-198.

Cusanelli, D.S., Hundley, L. (1999). Stern Flap Powering Performance on a *Spruance* Class Destroyer: Ship Trials and Model Experiments. *Naval Engineers Journal*, 111(2), 69-81.
De Roo, S., Vanhaute, L., Troch, P. (2012). Impact of ship waves on the sediment transport in a nature friendly bank protection. *River Flow* 2012, M. Murillo ed., Taylor & Francis, London.
Dean, R.G., Dalrymple R.A. (1991). *Water Wave Mechanics for Engineers and Scientists*. World Scientific Publishing, Singapore.
Froude, W. (1877). Experiments upon the effect produced on the wave-making resistance of ships by length of parallel middle body. *Trans. Inst. Naval Architects*, 18: 77-87.
Glamore, W. (2008) A Decision Support Tool for Assessing the Impact of Boat Wake Waves on Inland Waterways. *On-Course, PIANC*, October 2008, 5-18.
Ippen, A. ed. (1966). *Estuary and Coastline Hydrodynamics*. McGraw-Hill Book Company, New York.
LCH (2009). *Transport des déchets ménagers par voie navigable*. Report 09/2009, Laboratory of Hydraulic Constructions, Ecole Polytechnique Fédérale de Lausanne [unpublished].
LCH (2011). *Transport des déchets ménagers par voie navigable sur le Rhône: Efficacité des mesures anti-vagues.* Report 07/2011, Laboratory of Hydraulic Constructions, Ecole Polytechnique Fédérale de Lausanne [unpublished].
Le Méhauté, B. (1976). *An Introduction to Hydrodynamics and Water Waves*. Springer, New York.
Muk-Pavic, E., Chin, S.N., Spencer, D. (2006). Validation of the CFD code Flow-3D for the free surface flow around the ships' hulls. *14th Annual Conference of the CFD Society of Canada*.
Nanson, G.C., Krusenstierna, A., Bryant, E.A., Renilson, M.R. (1994). Experimental measurements on river-bank erosion caused by boat-generated waves on the Gordon River, Tasmania. *Regulated Rivers: Research & Management*, 9(1), 1-14.
Newman, J.N. (1977). *Marine Hydrodynamics*. MIT Press, Cambridge, UK.
Presles, D., Paulet, D. (2005). *Architecture navale, connaissance et pratique*. Éditions de la Villette, Paris.

AUTHOR BIOGRAPHIES

ROBIN AMACHER *is a naval architect and engineer. His activities relate to fluid dynamics ranging from the optimization of steering and propulsion systems to the design of foiling boats, such as the record-breaking catamaran"l'Hydroptère.ch".*

THÉODORA COHEN LIECHTI, PH.D. *is an environmental engineer who worked for five years as a research assistant at LCH of EPFL. Her areas of expertise are hydrological modeling, hydraulic engineering, and satellite-derived data analysis.*

MICHAEL PFISTER, DR.SC. *graduated in civil engineering, focusing on hydraulics. Presently, he is a Research and Teaching Associate at LCH of EPFL, conducting research mainly related to dam spillway hydraulics and high-speed two-phase air-water flows.*

GIOVANNI DE CESARE, DR.SC. *graduated in civil engineering. He is deputy director of the LCH of EPFL, Research and Teaching Associate and in charge of the hydraulic laboratory. His research focuses on physical and numerical modeling in all domains of hydraulic structures and schemes.*

PROFESSOR ANTON J. SCHLEISS, DR.SC. *is the director of the LCH of EPFL. The LCH activities comprise education, research, and services in the field of both fundamental and applied hydraulics and design of hydraulic structures and schemes.*